

22 **Abstract.** Two significant instrument biases have been identified in the in situ
23 profile data used to estimate globally integrated upper-ocean heat content. A large cold
24 bias was discovered in a small fraction of Argo floats along with a smaller but more
25 prevalent warm bias in eXpendable BathyThermograph (XBT) data. These biases appear
26 to have caused the bulk of the upper-ocean cooling signal reported by Lyman et al.
27 (2006) between 2003 and 2005. These systematic data errors are significantly larger than
28 sampling errors in recent years, and are the dominant sources of error in recent estimates
29 of globally integrated upper-ocean heat content variability. The bias in the XBT data is
30 found to be consistent with errors in the fall-rate equations, suggesting a physical
31 explanation for that bias. With biased profiles discarded, no significant warming or
32 cooling is observed in upper-ocean heat content between 2003 and 2006.

33 **1. Introduction**

34 As the Earth warms due to the buildup of greenhouse gasses in the atmosphere, the
35 vast majority of the excess heat is expected to go toward warming the oceans (Levitus et
36 al. 2005; Hansen et al. 2005). Changes in globally integrated upper ocean heat content
37 anomaly (OHCA) therefore have very important implications for understanding the
38 Earth's energy balance and the evolution of anthropogenic climate change.

39 A large and apparently significant cooling in OHCA between 2003 and 2005 was
40 reported by Lyman et al. (2006). It has been suggested that this cooling could be
41 attributed to transitioning from the warm-biased eXpendable BathyThermograph (XBT)
42 array and changes in sampling caused by the introduction of large amounts of data from
43 the Argo array of profiling floats (<http://www.argo.net>) in the Southern Ocean
44 (AchutaRao et al. 2007). However, an additional source of systematic data errors has
45 been discovered in a small number of Argo floats, which on balance, report temperature
46 profiles that appear spuriously cold. In the present analysis, the cooling reported by
47 Lyman et al. (2006) is shown to be an artifact caused by both the XBT warm bias and the
48 cold bias in the Argo data. Estimates of the sampling error based on altimeter data
49 suggest that changes in coverage did not contribute substantially to the spurious cooling
50 despite the rapid introduction of new data in the Southern Ocean from the Argo array.

51 A description of the systematic errors in the Argo data as well as their cause and
52 extent follows (Section 2). The warm bias in the XBT data during the period of the
53 cooling is discussed, and a possible explanation for its cause is presented (Section 3).
54 Finally, the effect of these biases on the OHCA estimate from 2003 through 2006 is
55 discussed (Section 4), followed by discussion and conclusions (Section 5).

56

57 **2. Argo Data Errors**

58 In the OHCA estimate of Lyman et al. (2006), rapid cooling was exhibited in the
59 tropical and subtropical Atlantic Ocean between 2003 and 2005. Comparison of
60 individual temperature profiles with historical data in this region uncovered significant
61 biases in profiles from a number of Argo floats (Figure 1). All of the affected profiles
62 were found in Argo real-time data, which had not undergone scientific quality control.

63 The data error occurs in SOLO (Sounding Oceanographic Lagrangian Observer)
64 instruments fabricated at WHOI (the Woods Hole Oceanographic Institution) and
65 equipped with either FSI (Falmouth Scientific, Inc.) or SBE (SeaBird Electronics, Inc.)
66 CTD (Conductivity-Temperature-Depth) sensors. Further investigation of the data
67 returned by these instruments uncovered a flaw that caused temperature and salinity
68 values to be associated with incorrect pressure values. The size of the pressure offset was
69 dependent on float type, varied from profile to profile and ranged from 2-5 db near the
70 surface to 10-50 db at depths below about 400 db. Almost all of the WHOI FSI floats
71 (287 instruments) and approximately half of the WHOI SBE floats (about 188
72 instruments) suffered from errors of this nature. The bulk of these floats were deployed
73 in the Atlantic Ocean, where the spurious cooling was found.

74 From Jan. 1, 2000 through June 30, 2007, the WHOI FSI floats produced
75 approximately 20,000 profiles, almost all of which contain spurious pressure values.
76 During the same period, WHOI SBE floats produced approximately 14,800 profiles,
77 about 7000 of which had pressure errors. These 30,000 spurious profiles account for
78 about 8 % of the total number of Argo profiles during this period.

79 Although errors in the affected profiles varied depending on float configuration,
80 their net effect was to produce a strong cold bias at depth. A regional mean of
81 temperature differences between the affected profiles and climatological temperature
82 from the WOCE Global Hydrographic Climatology (WGHC, Gouretski and Koltermann
83 2004) illustrates this (Figure 2). In contrast, the mean temperature anomaly based on
84 non-WHOI float data from the same region and time is smaller and positive. Data used
85 in Figure 2 were restricted to the Atlantic Ocean between 50°S and 50°N and from Jan. 1,
86 2003 to June 30, 2007. This includes about 24,200 of the biased profiles, and about
87 31,200 profiles from non-WHOI floats.

88 The cold bias is greater than -0.5°C between 400 and 700 m in the average over the
89 affected data and has a vertical structure that is similar to the cooling discussed in Lyman
90 et al. (2006). This structure is due primarily to the WHOI FSI floats, which assigned
91 incorrect pressure values that were predominantly biased shallow. Pressure offsets in the
92 affected WHOI SBE profiles were somewhat smaller and changed sign depending on
93 depth and float configuration.

94 It is important to note that these systematic errors were caused by improper
95 processing of data by a small subset of floats, and they do not reflect an inherent flaw in
96 the observing system. About one-half of the affected profiles have been corrected exactly
97 and the remainder will eventually be corrected to a good approximation. Corrected
98 profiles have been uploaded to the Global Data Archive Centers for a large number of the
99 floats. Profiles that have not been corrected are now flagged as “3 – bad data that are
100 potentially correctable,” in the variable “PRES_QC”. Further details regarding the status

101 of these data as well as complete lists of the affected floats may be found here:
102 http://www-argo.ucsd.edu/Acpres_offset2.html

103 These data cannot be easily repaired by the end user because correction requires
104 additional information reported by the floats, and is not a uniform offset over entire
105 profiles. Furthermore, the effect on an individual profile can be fairly small and difficult
106 to detect (Figure 2) without comparison to historical data and averaging over many
107 profiles. Therefore, profiles that remain uncorrected should be excluded from scientific
108 analyses that may be affected by pressure errors until corrected profiles become
109 available.

110

111 **3. XBT Instrument Bias**

112 Although XBT profiles account for a large fraction of historical ocean temperature
113 data since the late 1960s, these inexpensive instruments were not designed to provide
114 climate-quality scientific data. These probes do not measure pressure or depth, but
115 instead record temperature as a function of time since the probe entered the water. They
116 are designed to fall at a known rate, and fall-rate equations are used to convert elapsed
117 time into depth. The existence of systematic errors in the fall-rate equations provided by
118 the manufacturer have been known for some time and new fall-rate equations as well as a
119 correction factor for old XBT data have been estimated (Hanawa et al. 1995). Both here
120 and in Lyman et al. (2006), the corrections recommended by Hanawa et al. (1995) were
121 applied.

122 However, recent reports of time-dependent temperature biases in the XBT data
123 (Gouretski and Koltermann 2007) suggest that systematic errors in the fall-rate equations

124 may remain. Errors in the fall-rate equations result in temperatures that are assigned to
125 the incorrect depth. If temperature biases are related to the fall rate equations, then these
126 biases will be better explained by considering isotherm displacements, as attempted here.

127 For the data used by Lyman et al. (2006), isotherm displacements were computed
128 relative to the local temperature climatology as follows: $Z = (T - T_{\text{clim}}) / (\partial T_{\text{clim}} / \partial z)$. Here T is
129 observed temperature, T_{clim} is local climatological temperature from WGHC and dT_{clim}/dz
130 is the vertical temperature gradient, also computed from climatology. In order to test
131 whether warm biases in recent XBT data are consistent with a fall-rate error, XBT
132 profiles are compared with nearby Argo temperature profiles (excluding data from all
133 affected WHOI floats).

134 XBT/Argo pairs are defined to be within 4° longitude, 2° latitude, and 90 days in
135 time. This results in about 24,000 pairs from 2003 through the end of 2006. Regions
136 with vertical temperature gradients smaller than $0.002^{\circ}\text{C m}^{-1}$ were excluded. Median
137 differences between isotherm displacements computed from nearby XBT and Argo
138 profiles strongly suggest fall-rate errors (Figure 3). The isotherm displacements derived
139 from XBT probes are systematically deeper than Argo displacements by about 2% in the
140 median. The fact that this discrepancy approaches zero near the surface (outside of the
141 mixed layer) and increases linearly with depth suggests that the XBT bias is related to
142 incorrect calibration of the fall-rate equations, rather than an actual bias in temperature.

143 A similar comparison between isotherm displacements from Argo (excluding
144 WHOI float profiles) and CTD pairs from Jan. 1, 2000 through Dec. 31, 2006 (Figure 3)
145 shows no such pattern. Only about 2,300 Argo/CTD pairs were available, resulting in a
146 somewhat noisier estimate. However, the difference between displacements computed

147 from nearby CTD and Argo profiles is close to zero over most of the depth range
148 analyzed. The only range with large differences encompasses the surface mixed-layer,
149 where vertical temperature gradients can be small and temporal variations are large.
150 These two factors make the near-surface results noisy. The Argo/CTD comparison
151 suggests that once the WHOI float profiles have been removed, the remaining systematic
152 errors in the Argo data are much smaller than systematic errors in the XBT data.

153 Thus in the aggregate during the study period, XBT probes assign temperatures to
154 depths that are about 2% too deep (Figure 3). Despite the clear signal in the average, this
155 bias is small and difficult to detect in individual profiles, at either high or low latitudes
156 (Figure 3). It is important to note, however, that the median values presented here
157 represent an average over many different types of XBT instruments. Previous authors
158 have shown that fall-rate errors may vary depending on probe type (Hanawa et al. 1995)
159 and manufacturer (Kizu et al. 2005a, 2005b). Furthermore, misapplication of corrections
160 to fall-rate errors has compounded such problems in the past (Willis et al. 2004; Lombard
161 et al. 2004). Therefore, we caution against application of any depth correction on the
162 basis of the results presented here. However, a detailed analysis of XBT fall-rate errors
163 and their dependence on time and probe type was recently completed (Wijffels et al.
164 2008). The 2% error in depth presented here is in good agreement with their findings for
165 the period considered here.

166

167 **4. Recent OHCA Variability**

168 The effects of these systematic data errors on OHCA estimates between 2003 and
169 2006 are demonstrated using subsets of the profile data. These subsets were used to

170 compute yearly maps of OHCA in manner of (Willis et al., 2004), which were spatially
171 integrated to produce OHCA time series (Figure 4).

172 Error bars (Figure 4) are computed as in Lyman et al. (2006) using the multi-
173 satellite estimate of sea surface height anomaly (SSH) from AVISO (Ducet et al. 2000).
174 These error bars represent sampling error only and there may be additional uncertainties,
175 most notably from instrument biases and inaccuracies in the climatology. Because the
176 satellite altimeters provide near-global coverage during this period, and since numerous
177 studies (White and Tai 1995; Gilson et al. 1998; Willis et al. 2003; 2004) have
178 demonstrated the strong relationship between SSH anomaly and OHCA or thermosteric
179 sea level anomaly (Zang and Wunsch 2001, their figure 6), altimeter data can be used as a
180 proxy for testing the effects of in situ data sampling on estimates of globally averaged
181 OHCA.

182 The OCHA estimate made using all data including spurious float profiles (thick
183 solid line) shows an apparent cooling of 77×10^{21} J from 2003 to 2006. Another estimate
184 using all data except the spurious float profiles (thick dashed line) suggests much less
185 cooling, only about 41×10^{21} J. More than half of the erroneous cooling arises because
186 of the increasing fraction of spurious profiles in the Argo data stream produced by the
187 WHOI floats, primarily the floats with FSI instruments.

188 The effect of the XBT bias is demonstrated by making OHCA estimates from two
189 more subsets of the data. The first is made using only Argo data but excluding the
190 spurious WHOI profiles (Figure 4, thin solid line). This ‘Argo-only’ estimate shows no
191 significant warming or cooling between 2003 and 2006, with a decrease of only $-4 (\pm 18)$

192 $\times 10^{21}$ J during this period. This estimate of OHCA variability is the most robust during
193 this short time interval.

194 The final OHCA estimate is made by excluding all Argo float data (Figure 4, thin
195 dashed line), and consists primarily of XBT profiles that are uncorrected for the fall-rate
196 bias shown in Figure 3. The amount of non-Argo data is small during these years and
197 large gaps exist in the data coverage for this estimate of OHCA. This is reflected by the
198 $20 - 30 \times 10^{21}$ J sampling error bars for this estimate (Figure 4). Although it is not a
199 robust estimate of OHCA, this ‘XBT-only’ estimate is 75×10^{21} J warmer than the Argo-
200 only estimate and lies well outside the sampling error bars of either estimate. This large
201 separation exists despite the paucity of data in the XBT-only estimate and the fact that the
202 mapping procedure causes both estimates to relax to the same mean in regions with little
203 data. We note that this positive offset was not visible in Lyman et al. (2006) because in
204 that study, record-length means were subtracted from the two different OHCA estimates
205 before plotting.

206 The reason for the apparent cooling in the estimate that combines both XBT and
207 Argo data (thick dashed line) is the increasing ratio of Argo observations to XBT
208 observations between 2003 and 2006. This changing ratio causes the combined estimate
209 to exhibit cooling as it moves away from the warm-biased XBT data and toward the more
210 neutral Argo values.

211 In order to test the suggestion by AchutaRao et al. (2007) that increased sampling
212 in the Southern Ocean from the Argo array was partly responsible for the spurious
213 cooling, an experiment was conducted using the AVISO data as a proxy for OHCA. The
214 technique was similar to the one used to determine the sampling error (Lyman et al.

215 2006). Altimetric height was first subsampled by interpolating to the time and location of
216 each profile. The subsampled data were then mapped using the same mapping procedure
217 as that of the OHCA estimates. The resulting maps of altimetric height were globally
218 averaged and compared with the globally averaged AVISO maps (Figure 5). This
219 exercise illustrates the effect of the changing in situ data distribution on estimates of the
220 global average. Although the subsampled estimate dips slightly farther below the fully
221 sampled estimate between 2003 and 2004, it increases more rapidly than the fully
222 sampled estimate between 2005 and 2006. It should be noted that SSH is only a proxy
223 for OHCA, as it contains deep water, fresh water, and mass signals that are not in upper
224 OHCA. Nevertheless, this result suggests that the increased sampling of the Southern
225 Ocean by the Argo array did not cause a significant bias in the OHCA estimates. This
226 finding is consistent with those of Lyman and Johnson (2008), who present a more
227 detailed look at the effect of historical in situ sampling patterns on OHCA in the context
228 of AVISO SSH.

229

230 **5. Discussion and Conclusions**

231 Systematic pressure errors have been identified in real-time temperature and
232 salinity profiles from a small number of Argo floats. These errors were caused by
233 problems with processing of the Argo data, and corrected versions of many of the
234 affected profiles have been supplied by the float provider. Profiles that remain
235 uncorrected, however, may be unsuitable for many oceanographic analyses. Recent
236 scientific results that relied heavily on real-time Argo data in the tropical and subtropical
237 Atlantic downloaded prior to October 31, 2007 (W. B. Owens and C. Schmid, personal

238 communication 2007) may require re-examination for sensitivity to these errors. Argo
239 data users should be aware that real-time Argo data only undergo rudimentary checks,
240 and only delayed-mode Argo data have undergone rigorous quality control and been
241 examined by the float providers. Although details will vary depending on the
242 application, users of real time Argo data may wish to apply quality control procedures
243 such as those described by Willis et al. (2008) for making estimates of globally averaged
244 quantities such as globally averaged OHCA or steric sea level.

245 Most of the rapid cooling reported by Lyman et al. (2006) is demonstrated to be the
246 result of the combination of this cold bias in the spurious Argo data and the transition
247 from an ocean observing system dominated by warm-biased XBT data to one dominated
248 by Argo data. Furthermore, these systematic errors are shown to be significantly larger
249 than estimated sampling errors in OHCA. It is also shown that sampling changes from
250 the Argo array in the Southern Ocean are unlikely to have made a significant contribution
251 to the spurious cooling.

252 OHCA does not appear to exhibit significant warming or cooling between 2003 and
253 2006. However, without fully addressing the XBT bias, it does not seem prudent to
254 combine XBT data with data from the Argo array to produce a long-term estimate of
255 OHCA. Furthermore, only in 2003 does Argo coverage become adequate to determine
256 the global integral without including XBT profiles. For these reasons, OHCA variability
257 is not estimated prior to 2003 in the present analysis.

258 Here errors in the fall-rate equations are proposed to be the primary cause of the
259 XBT warm bias. For the study period, XBT probes are found to assign temperatures to
260 depths that are about 2% too deep. In the global integral, this fall-rate error is consistent

261 with results here that XBT-based OHCA estimates are biased warm by about 73×10^{21} J
262 relative to Argo-based estimates during this period.

263 The cooling reported by Lyman et al. (2006) would have implied a very rapid
264 increase in the rate of ice melt in order to account for the fairly steady increase in global
265 mean sea level rise observed by satellite altimeters over the past several years. The
266 absence of a significant cooling signal in the OHCA analyses presented here brings
267 estimates of upper-ocean thermosteric sea level variability into closer agreement with
268 altimeter-derived measurements of global mean sea level rise. Nevertheless, some
269 discrepancy remains in the globally averaged sea level budget and observations of the
270 rate of ocean mass increase and upper-ocean warming are still too small to fully account
271 for recent rates of sea level rise (Willis et al. 2008). Temperature changes in the deep
272 ocean (e.g. Johnson et al. 2008) may account for some of that discrepancy, at least over
273 multi-decadal time-scales (Domingues et al., 2008).

274

275 **Acknowledgments.** The bulk of the in situ data used herein were provided through the
276 World Ocean Database 2001 and the Global Temperature-Salinity Profile Program
277 (<http://www.nodc.noaa.gov>). Float data were collected and made freely available by
278 Argo (a pilot program of the Global Ocean Observing System) and contributing national
279 programs (<http://www.argo.net/>). Altimeter products used herein were produced by
280 Ssalto/Duacs as part of the Environment and Climate EU Enact project (EVK2-CT2001-
281 00117) and distributed by Aviso, with support from CNES. This research was carried out
282 in part at the Jet Propulsion Laboratory, California Institute of Technology, under a
283 contract with the National Aeronautics and Space Administration. JML and GCJ were

284 supported by the NOAA Climate Program Office and the NOAA Office of Oceanic and
285 Atmospheric Research. Comments from multiple anonymous reviewers improved the
286 manuscript. The findings and conclusions in this article are those of the authors and do
287 not necessarily represent the views of the National Oceanic and Atmospheric
288 Administration.

289 **References**

- 290 AchutaRao, K. M., M. Ishii, B. D. Santer, P. J. Gleckler, K. E. Taylor, T. P. Barnett, D.
291 W. Pierce, R. J. Stouffer, and T. M. L. Wigley (2007): Simulated and observed
292 variability in ocean temperature and heat content. *Proc. Natl. Acad. Sci.*, **104** (26)
293 10768–10773, doi:10.1073/pnas.0611375104.
- 294 Barnett, T. P., D. W. Pierce, K. AchutaRao, P. J. Gleckler, B. D. Santer, J. M. Gregory,
295 and W. M. Washington (2005): Penetration of human-induced warming into the
296 world’s oceans. *Science*, **309**, 284–287, doi:10.1126/science.1112418.
- 297 Domingues, C. M., J. A. Church, N. J. White, P. J. Gleckler, S. E. Wijffels, P. M. Barker,
298 and J. R. Dunn (2008), Improved estimates of upper-ocean warming and multi-
299 decadal sea-level rise. *Nature*, **453**, 1090-1093.
- 300 Douglass, E., D. Roemmich, and D. Stammer (2006): Interannual variability in northeast
301 Pacific circulation. *J. Geophys. Res.*, **111**, C04001, doi:10.1029/2005JC003015.
- 302 Ducet, N., P.-Y. Le Traon, G. Reverdin (2000): Global high-resolution mapping of ocean
303 circulation from TOPEX/Poseidon and ERS-1 and -2. *J. Geophys. Res.*, **105**,
304 19,477–19,898, doi:10.1029/2000JC900063.
- 305 Gilson, J., D. Roemmich, B. Cornuelle, and L.-L. Fu (1998): Relationship of
306 TOPEX/Poseidon altimetric height to steric height and circulation of the North
307 Pacific. *J. Geophys. Res.*, **103**, 27,947–27,965.
- 308 Gouretski, V. V., and K. P. Koltermann (2004): WOCE global hydrographic climatology
309 [CD-ROM]. *Ber. Bundesamt Seeschifffahrt Hydrogr. Rep.*, 35, 52 pp., Bundesamt
310 Seeschifffahrt Hydrogr., Hamburg, Germany.

311 Gouretski V., K. P. Koltermann (2007): How much is the ocean really warming?
312 *Geophys. Res. Lett.*, **34**, L01610, doi:10.1029/2006GL027834.

313 Hanawa, K., P. Rual, R. Bailey, A. Sy, and M. Szabados (1995): A new depth-time
314 equation for Sippican or TSK T-7, T-6, and T-4 expendable bathythermographs
315 (XBT). *Deep-Sea Res. I*, **42**, 1423–1451.

316 Hansen, J., L. Nazarenko, R. Ruedy, M. Sato, J. Willis, A. Del Genio, D. Koch, A. Lacis,
317 K. Lo, S. Menon, T. Novakov, J. Perlwitz, G. Russell, G. A. Schmidt, and N.
318 Tausnev (2005): Earth's energy imbalance: Confirmation and implications. *Science*,
319 **308**, 1431-1435.

320 Johnson, G. C., S. Mecking, B. M. Sloyan, and S. E. Wijffels. 2007. Recent bottom water
321 warming in the Pacific Ocean. *J. Clim.*, **20**, 5365-5375.

322 Kizu, S., S.-I. Ito, and T. Watanabe (2005a): Inter-manufacturer Difference and
323 Temperature Dependency of the Fall-Rate of T-5 Expendable Bathythermograph.
324 *J. Oceanogr.*, **61**, 905-912.

325 Kizu, S., H. Yoritaka and K. Hanawa (2005b): A new fall-rate equation for T-5
326 expendable bathythermograph (XBT) by TSK. *J. Oceanogr.*, **61**, 115–121.

327 Levitus, S. J., I. Antonov, and T. P. Boyer (2005): Warming of the world ocean, 1955 –
328 2003. *Geophys. Res. Lett.*, **32**, L02604, doi:10.1029/2004GL021592.

329 Lombard. A., A. Cazenave, P.-Y. Le Traon, M. Ishii (2004): Contribution of thermal
330 expansion to present-day sea-level change revisited. *Global Planet. Change*, **47**,
331 1-16.

332 Lyman, J.M. and G. C. Johnson (2008): Estimating Annual Global Upper Ocean Heat
333 Content Anomalies Despite Irregular In Situ Ocean Sampling. *J. Clim.*, in press,
334 doi:10.1175/2008JCLI2259.1. .

335 Lyman, J. M., J. K. Willis, G. C. Johnson (2006): Recent Cooling in the Upper Ocean.
336 *Geophys. Res. Lett.*, **33**, L18604, doi:10.1029/2006GL027033.

337 Stephens, C., J. I. Antonov, T. P. Boyer, M. E. Conkright, R. A. Locarnini, T. D.
338 O'Brien, and H. E. Garcia (2002): World ocean atlas 2001, volume 1:
339 Temperature. *Tech. Rep., Atlas NESDIS 49*, 167 pp., Natl. Ocean and Atmos.
340 Admin., Washington, D.C.

341 White, W., and C.-K. Tai (1995): Inferring interannual changes in global upper ocean
342 heat storage from TOPEX altimetry, *J. Geophys. Res.*, *100*, 24943-24954.

343 Wijffels S. E., Willis J., Domingues C. M., Barker P., White N. J., et al. (2008):
344 Changing eXpendable Bathythermograph Fall-rates and their Impact on Estimates
345 of Thermosteric Sea Level Rise, *J. Clim.*, In Press.

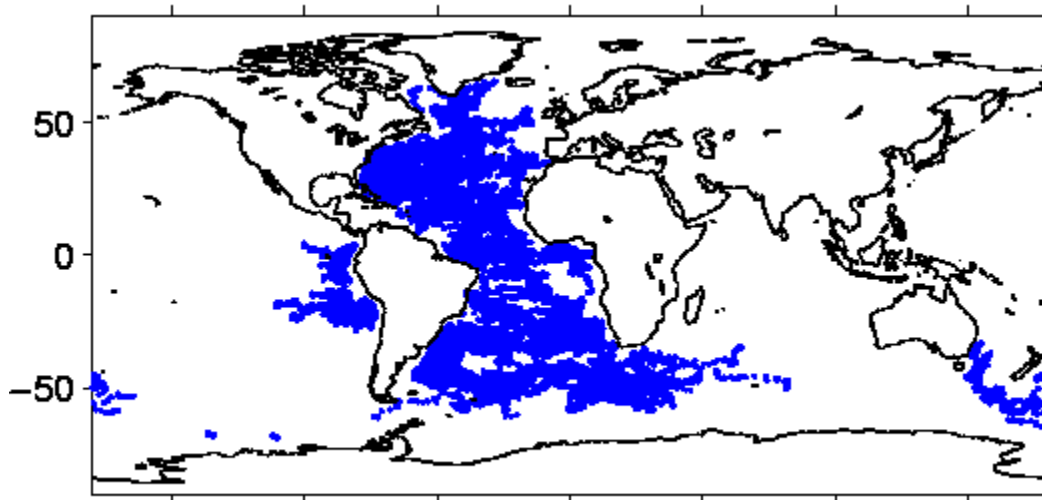
346 Willis, J. K., D. Roemmich, and B. Cornuelle (2003): Combining altimetric height with
347 broadscale profile data to estimate steric height, heat storage, subsurface
348 temperature, and sea-surface temperature variability, *J. Geophys. Res.*, *108*, 3292.

349 Willis, J. K., D. Roemmich, and B. Cornuelle (2004): Interannual variability in upper
350 ocean heat content, temperature, and thermosteric expansion on global scales. *J.*
351 *Geophys. Res.*, **109**, C12036, doi:10.1029/2003JC002260.

352 Willis, J. K., D. P. Chambers, and R. S. Nerem (2008), Assessing the globally averaged
353 sea level budget on seasonal to interannual timescales, *J. Geophys. Res.*, *113*,
354 C06015, doi:10.1029/2007JC004517.

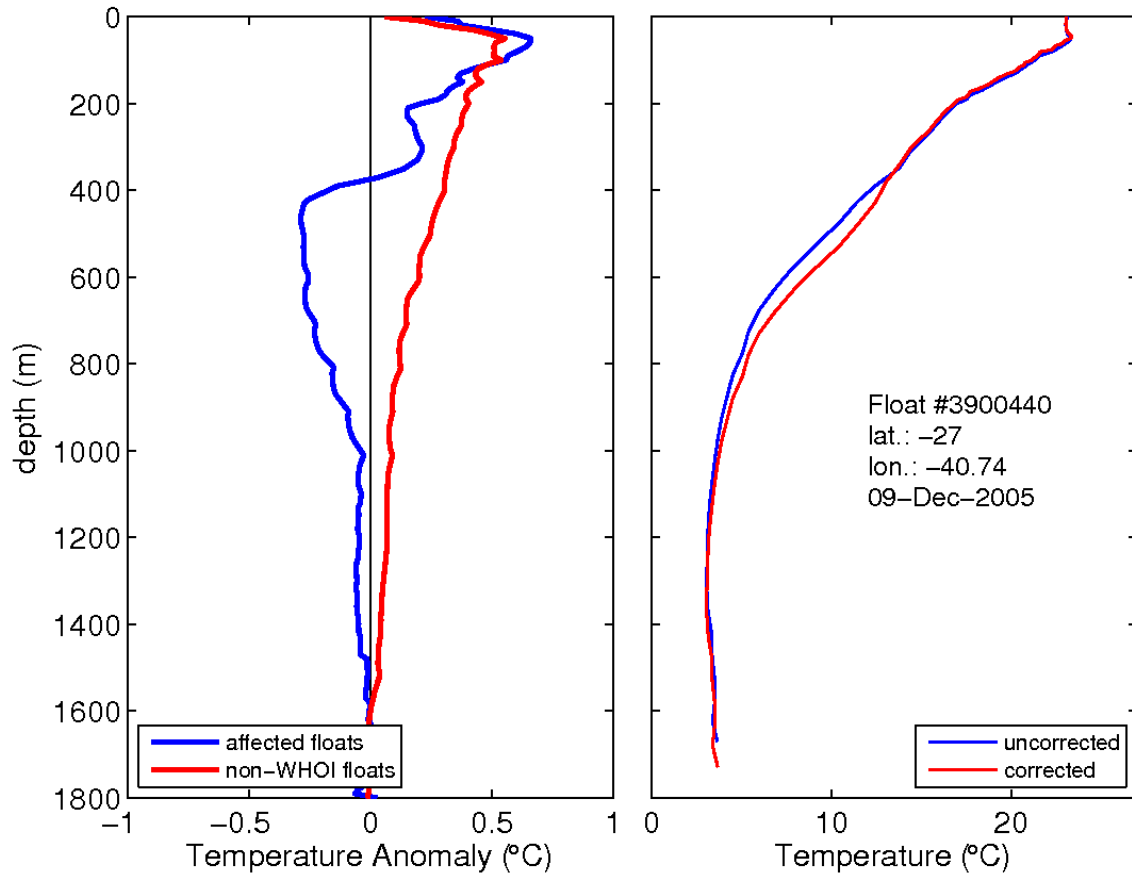
355 Zang, X., and C. Wunsch (2001): Spectral description of low-frequency oceanic
356 variability. *J. Phys. Oceanogr.*, **31**(10), 3,073-3,095.

357 **Figures**



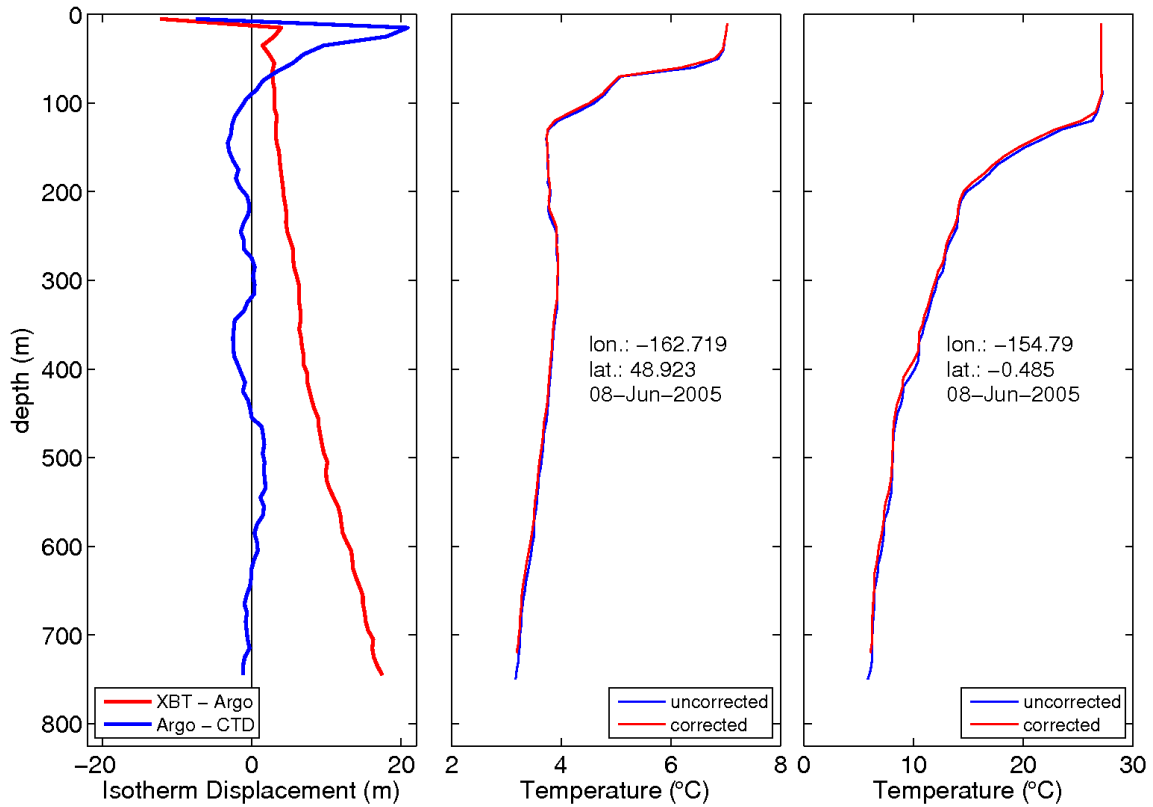
358

359 **Figure 1.** Distribution of profiles from WHOI floats with spurious pressure values
360 reported from January 1, 2003 through June 30, 2007.



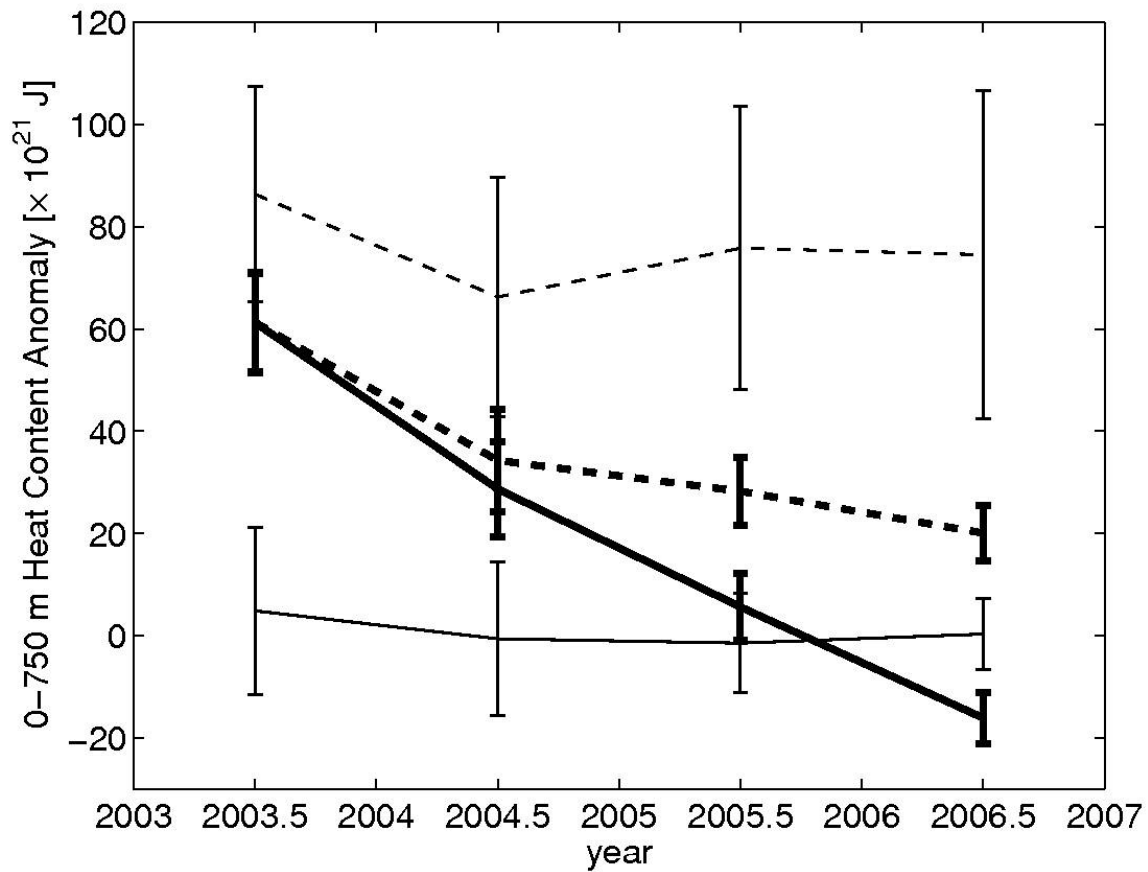
361

362 **Figure 2.** Left panel: Temperature anomaly versus depth relative to the WGHC for
 363 WHOI floats with incorrect pressure values (blue line) and non-WHOI floats from the
 364 same region (red line). Data were restricted to the Atlantic and to latitudes between 50°S
 365 and 50°N from Jan. 1, 2003 through June 30, 2007. Right panel: Effect of the correction
 366 for a single float WHOI FSI float in the South Atlantic.



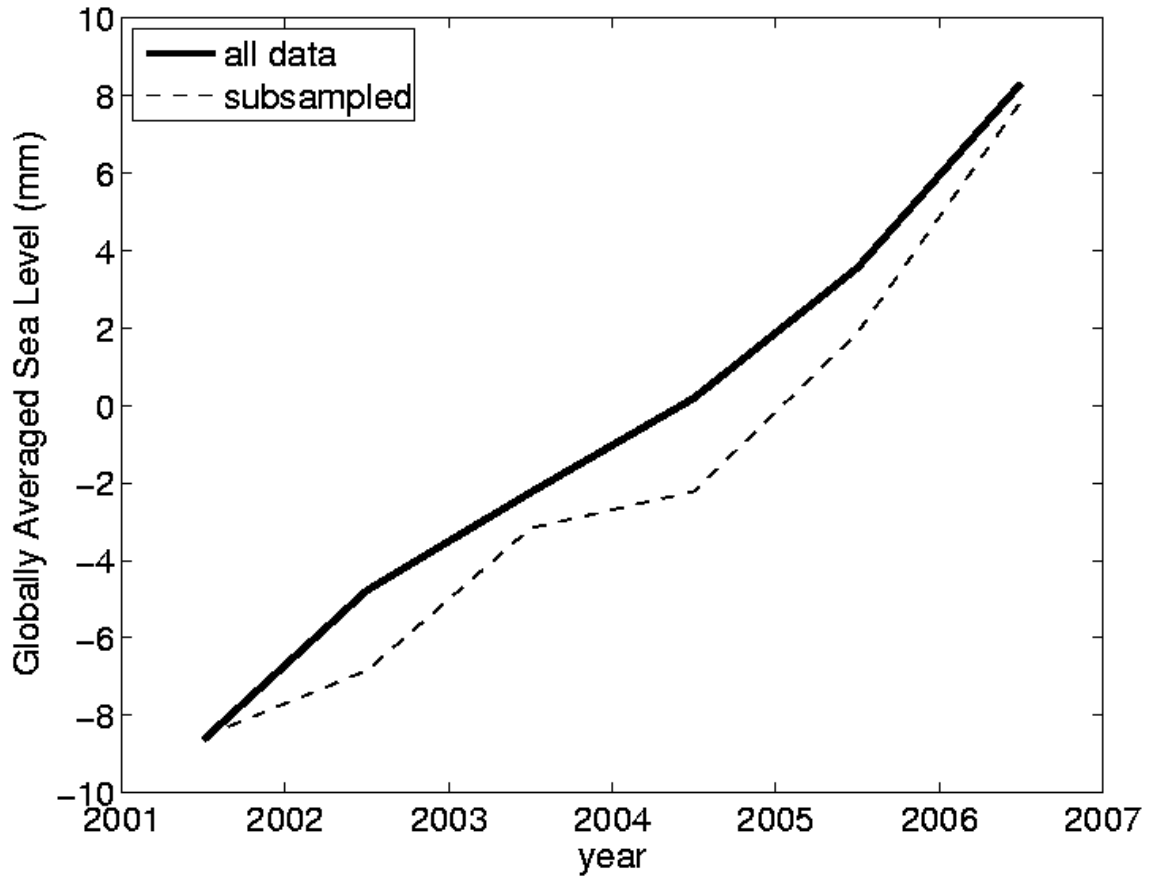
367

368 **Figure 3.** Left panel: Median difference between isotherm displacements computed from
 369 24,000 nearby XBT and Argo pairs collected between Jan. 1, 2003 and Dec. 31, 2006
 370 (red line). Also shown is the median difference between isotherm displacements
 371 computed from 2,300 nearby CTD and Argo pairs collected between Jan. 1, 2000 and
 372 Dec. 31, 2006 (blue line). All WHOI floats were excluded from this analysis. Positive
 373 displacements reflect deeper isotherms. Middle and right panels: Effect of a 2% bias on
 374 two individual profiles in the North Pacific (center panel) and Tropical Pacific (right
 375 panel).



377

378 **Figure 4.** Annual values of globally integrated OHCA in the upper 750 m using all
 379 available data (thick solid line), using all data except profiles from WHOI floats with
 380 spurious pressure values (thick dashed line), using only Argo data except profiles from
 381 affected WHOI floats (thin solid line), and using no Argo data (thin dashed line). As in
 382 Lyman et al. (2006), error bars reflect only sampling errors and not the complete error
 383 budget.



384
 385 **Figure 5.** Globally averaged sea level from altimeter data. Comparing sea level
 386 estimated by averaging over the AVISO maps of SSH (solid line) versus that from
 387 AVISO data subsampled at in situ data locations, mapped, and globally averaged (dashed
 388 line) illustrates the effect of changing in situ data distributions during the spin-up of the
 389 Argo array on estimates of the global mean.